

Dominant $(g_{9/2})^2$ neutron configuration in the 4_1^+ state of ^{68}Zn based on new g factor measurements

J. Leske^a, K.-H. Speidel^a, S. Schielke^a, J. Gerber^b,
P. Maier-Komor^c, T. Engeland^d, M. Hjorth-Jensen^d

^a*Helmholtz-Institut für Strahlen und Kernphysik, Universität Bonn, Nussallee 14-16, D-53115 Bonn, Germany*

^b*Institut de Recherches Subatomiques, F-67037 Strasbourg, France*

^c*Physik-Department, Technische Universität München, James-Frank-Str., D-85748 Garching, Germany*

^d*Department of Physics and Center of Mathematics for Applications, University of Oslo, N-0316 Oslo, Norway*

Abstract

The g factor of the 4_1^+ state in ^{68}Zn has been remeasured with improved energy resolution of the detectors used. The value obtained is consistent with the previous result of a negative g factor thus confirming the dominant $0g_{9/2}$ neutron nature of the 4_1^+ state. In addition, the accuracy of the g factors of the 2_1^+ , 2_2^+ and 3_1^- states has been improved and their lifetimes were well reproduced. New large-scale shell model calculations based on a ^{56}Ni core and an $0f_{5/2}1pg_{9/2}$ model space yield a theoretical value, $g(4_1^+) = +0.008$. Although the calculated value is small, it cannot fully explain the experimental value, $g(4_1^+) = -0.37(17)$. The magnitude of the deduced $B(E2)$ of the 4_1^+ and 2_1^+ transition is, however, rather well described. These results demonstrate again the importance of g factor measurements for nuclear structure determinations due to their specific sensitivity to detailed proton and neutron components in the nuclear wave functions.

Key words: g factors and lifetimes; ^{68}Zn , projectile Coulomb excitation; Inverse kinematics; Transient Field and DSAM

PACS: 21.10.Ky; 25.70.De; 27.50.+e

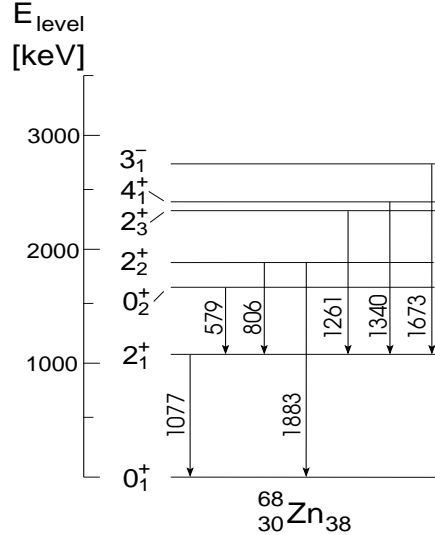


Fig. 1. Level scheme of ^{68}Zn with γ transitions relevant to the present work.

1 Introduction

Measurements of nuclear magnetic dipole and electric quadrupole moments provide valuable insights into the nuclear structure based on the intriguing interplay of single particle and collective degrees of freedom. In particular, nuclei in the *sd*- and *fp*-shell model space have recently received considerable attention through many new experiments inspired by the unique possibility to compare extensive data with results from large-scale shell model calculations. This progress is also related with the observation that general features of the nuclear medium can be studied in lighter nuclei as well. For instance, superdeformation which had been exclusively investigated for a long time on nuclei in the rare earth mass region and beyond [1] has recently been observed in ^{36}Ar [2], ^{40}Ca [3], ^{60}Zn [4] and ^{62}Zn [5]. The obvious advantage in all these cases is the possibility to directly compare data with structure calculations based on highly developed nuclear shell model codes thus providing new features of this phenomenon and collectivity in general on a microscopic non-phenomenological level.

In the same context measurements of g factors and $B(E2)$ values have been carried out for even- A Zn isotopes with $A = 62 - 70$ [6]. Two sets of large-scale shell model calculations were applied, based either on a ^{40}Ca core and an *fp*-shell model space or a ^{56}Ni core and an *fp g* -shell configuration space with the inclusion of the $0g_{9/2}$ orbital; the latter was considered to be particularly important for the heavier Zn isotopes. In these measurements Coulomb excitation of 160 MeV Zn projectiles was achieved in collisions with a carbon target employing inverse kinematics. At this beam energy essentially the first 2^+ states were strongly excited whereas higher-lying states were only weakly populated.

This deficiency was overcome in a succeeding experiment aiming at higher

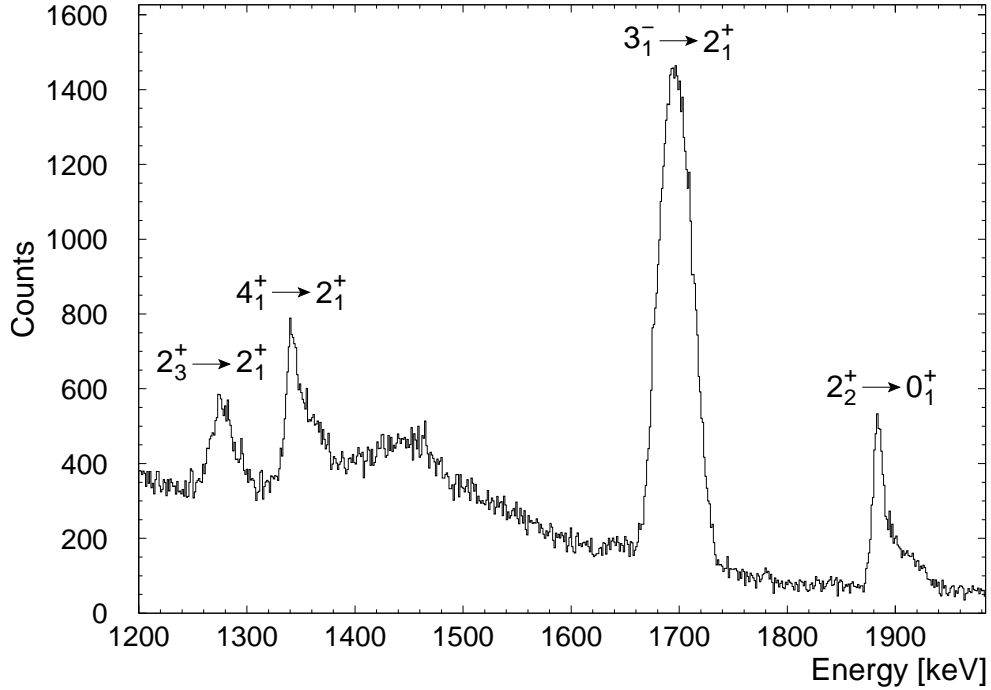


Fig. 2. Relevant γ -coincidence spectrum of a Ge detector placed at $\Theta_\gamma=65^\circ$ relative to the beam axis. The Doppler-broadened lineshapes reflect the nuclear lifetimes.

excitation energies of both ^{64}Zn and ^{68}Zn by increasing the projectile energies to 180 MeV close to the Coulomb barrier [7]. In these new measurements the g factors and the $B(E2)$ values of the now accessible 4_1^+ states were determined for the first time. Whereas the $g(4_1^+)$ value of ^{64}Zn was found to be consistent with predictions of both the collective and the spherical shell model, the value for ^{68}Zn of $g(4_1^+) = -0.4(2)$ turned out to be in severe conflict with both model predictions. The negative sign of the g factor was a clear indication for a dominant $0g_{9/2}$ neutron component in the wave function, whereby the Schmidt value is $g_{\text{Schmidt}} = -0.467$ which, however, was not verified by the calculations. On the other hand, the newly determined $B(E2)$ values were very well explained by these shell model calculations based on a ^{56}Ni core plus $0g_{9/2}$ neutrons. Evidently, in this case the explicit inclusion of the $0g_{9/2}$ orbital seems to be crucial for ^{68}Zn , as the alternative calculations, assuming an inert ^{40}Ca core but excluding the $0g_{9/2}$ orbital, underestimate the experimental E2 strength.

In order to set the g factor result of the $^{68}\text{Zn}(4_1^+)$ state on more solid grounds new measurements have been performed. As emphasized in [7] such an effort is required as in the previous measurements the energy resolution of the NaI(Tl) scintillators used for γ detection did not allow to fully separate the relevant ($4_1^+ \rightarrow 2_1^+$) γ line from a neighbouring ($2_3^+ \rightarrow 2_1^+$) 1261 keV line. As the latter was also strongly Doppler-shifted due to the short nuclear lifetime, the sepa-

ration of the two γ lines was particularly crucial for the detector pair placed in the forward hemisphere. On the other hand, estimates of an eventual admixture of the 2_3^+ state to the measured precession of the 4_1^+ state, based on the observed line intensities and the angular correlations of the corresponding γ transitions, could not explain the deduced g factor, even under the assumption of a negative g value for the 2_3^+ state.

2 Experimental details

In the present experiment a beam of isotopically pure ^{68}Zn ions was accelerated to an energy of 180 MeV at the Munich tandem accelerator providing intensities of 20 enA on a multilayered target. The latter consisted of 0.44 mg/cm² natural carbon deposited on a 3.34 mg/cm² Gd layer, which was evaporated on a 1.4 mg/cm² Ta foil, backed by a 4.49 mg/cm² Cu layer. Between C and Gd as well as between Ta and Cu thin layers of natural titanium (~ 0.005 mg/cm²) provided good adherence being very crucial for the precession experiments. The same target had been used in former measurements under almost identical conditions [7]. The target was cooled to liquid nitrogen temperature and magnetized to saturation by an external field of 0.06 T. The relevant level scheme of ^{68}Zn for Coulomb excitation is shown in Fig. 1 [8]. The excited Zn nuclei move through the Gd layer at mean velocities of $\sim 5.9v_0$ ($v_0 = e^2/\hbar$) experiencing spin precessions in the transient field and are ultimately stopped in the hyperfine-interaction-free environment of the Cu backing.

The de-excitation γ rays were measured in coincidence with the forward scattered carbon ions detected in a 100 μm Si detector at 0° . A 5 μm thick Ta foil between target and particle detector served as a beam stopper which, however, was transparent to the carbon recoils. As in the previous experiments the detector was operated at a very low bias of ~ 5 V to establish a thin depletion layer for separating the energies of carbon ions from those of light particles as protons and α particles resulting from sub-Coulomb fusion and transfer reactions. Under these conditions very clean γ -coincidence spectra were obtained. Intrinsic Ge detectors of $\sim 40\%$ relative efficiency were used for γ detection. Fig. 2 shows a typical coincidence spectrum with emphasis on the ($4_1^+ \rightarrow 2_1^+$) γ line. Evidently, all relevant γ lines were well resolved allowing a rigorous determination of their intensities required for the angular correlations as well as for the precessions of the nuclear states in question.

Particle- γ angular correlations $W(\Theta_\gamma)$ have been measured for determining the slope $|S| = [1/W(\Theta_\gamma)] \cdot [dW(\Theta_\gamma)/d\Theta_\gamma]$ in the rest frame of the γ emitting nuclei at $\Theta_\gamma^{lab} = \pm 65^\circ$ and $\pm 115^\circ$, where the sensitivity to the precessions was optimal for all transitions of interest. Precession angles, Φ^{exp} , were derived from counting-rate ratios 'R' for 'up' and 'down' directions of the external

magnetizing field which can be expressed as [7] ,

$$\Phi^{exp} = \frac{1}{S} \cdot \frac{\sqrt{R} - 1}{\sqrt{R} + 1} = g \frac{\mu_N}{\hbar} \int_{t_{in}}^{t_{out}} B_{TF}(v_{ion}(t)) e^{-\frac{t}{\tau}} dt \quad (1)$$

where g is the g factor of the nuclear state and B_{TF} the transient field acting on the nucleus during the time interval $(t_{out} - t_{in})$ which the ions spend in the gadolinium layer of the target; the exponential accounts for nuclear decay with lifetime τ in the Gd layer.

Simultaneously with the precessions the lifetimes of several excited states have been redetermined using the Doppler-Shift-Attenuation-Method (DSAM). For the analysis of the Doppler-broadened lineshapes, which were observed with a Ge detector placed at 0° to the beam direction, the computer code LINE-SHAPE [9] has been used. Specific details of the analysis procedure are given in [6,7].

3 Results and discussion

The g factors have been determined from the measured precession angles by calculating the effective transient field B_{TF} on the basis of the empirical linear parametrization (see [6,7]):

$$B_{TF}(v_{ion}) = G_{beam} \cdot B_{lin}, \quad (2)$$

with

$$B_{lin} = a(Gd) \cdot Z_{ion} \cdot v_{ion}/v_0, \quad (3)$$

where the strength parameter $a(Gd) = 17(1)T$ [7], and $G_{beam} = 0.61(6)$ is the attenuation factor accounting for the demagnetization of the Gd layer induced by the Zn beam (see [7]). The same scheme has been successfully applied in many former measurements. Precession and lifetime data from a single run are summarized in Table 1 together with the deduced g factors which are compared with previous results [7]. Evidently, all newly determined lifetimes and g factors are in good agreement with earlier data [7]. Furthermore, the g factor of the 4_1^+ state with its negative sign is confirmed whereby the relatively large error in the magnitude is of purely statistical origin due to the small excitation cross-section of the nuclear state and the low γ -detection efficiency of the Ge detectors. The striking difference in the g factors of the 4_1^+ states between ^{64}Zn and ^{68}Zn is shown in Fig. 3.

Table 1

Summary of the measured slopes of the angular correlations at $\Theta_\gamma^{Lab}=\pm 65^\circ$, precession angles and lifetimes of excited states in ^{68}Zn . The Φ_{lin}/g values were calculated using Eqs.(1)-(3). The g factors deduced and the newly determined lifetimes are compared with previous results [7].

E_x [MeV]	I^Π	τ [ps]		$ S(65^\circ) $ [$mrad$] ⁻¹	Φ^{exp} [mrad]	Φ^{lin}/g [mrad]	$g(I)$	
		present	[7]				present	[7]
1.077	2_1^+	2.34(4)	2.32(5)	2.133(15)	15.2(2)	26.4(26)	+0.58(6)	+0.50(5)
1.883	2_2^+	1.5(1)	1.4(1)	1.24(16)	12(4)	24.9(25)	+0.48(17)	+0.53(16)
2.338	2_3^+	0.47(6)	0.45(4)	–	–	–	–	–
2.417	4_1^+	1.18(8)	1.10(8)	0.85(18)	–6(8)	23.8(24)	–0.3(3)	–0.4(3)
2.751	3_1^-	0.37(1)	0.38(2)	0.310(52)	5(6)	16.7(17)	+0.3(4)	+0.4(4)

Table 2

Comparison of experimental excitation energies, average g factors and $B(E2)$ values (see also [7]) of $^{64,68}\text{Zn}$ with results from shell-model calculations (see text for further details).

Nucleus	$E(I_f^\pi)$ [MeV]			$I_f^\pi \rightarrow I_i^\pi$	$\tau(I_f^\pi)$ [ps]	$g(I_f^\pi)$		
	exp.	SM-1	SM-2			exp.	SM-1	SM-2
^{64}Zn	0.992		1.057	$2_1^+ \rightarrow 0_1^+$	2.77(6)	+0.446(25)		+0.813
	3.207		2.830	$4_1^+ \rightarrow 2_1^+$	1.12(4)	+0.53(16)		+1.568
	1.799		2.467	$2_2^+ \rightarrow 0_1^+$	2.9(3)	–		+0.334
^{68}Zn	1.077	0.765	0.934	$2_1^+ \rightarrow 0_1^+$	2.33(3)	+0.498(26)	+0.027	+0.223
	2.417	1.936	2.097	$4_1^+ \rightarrow 2_1^+$	1.14(6)	–0.37(17)	+0.066	+0.008
	1.883	1.318	1.629	$2_2^+ \rightarrow 0_1^+$	1.45(7)	+0.51(11)	+0.672	+0.242

In Table 2, the g factors and the $B(E2)$'s, both improved in accuracy by averaging with the data of [6,7], are compared with results from large-scale shell model calculations.

In order to study the importance of the $0g_{9/2}$ orbit we have performed shell model calculations using ^{56}Ni as closed shell core, with a model space defined by protons and neutrons occupying the single-particle orbitals $0f_{5/2}$, $1p_{3/2}$, $1p_{1/2}$ and $0g_{9/2}$ ($0f_{5/2}1pg_{9/2}$). To determine the effective interaction we use the recent charge-dependent potential model of Machleidt, the so-called CD-Bonn interaction [11]. The final effective two-body interaction is obtained

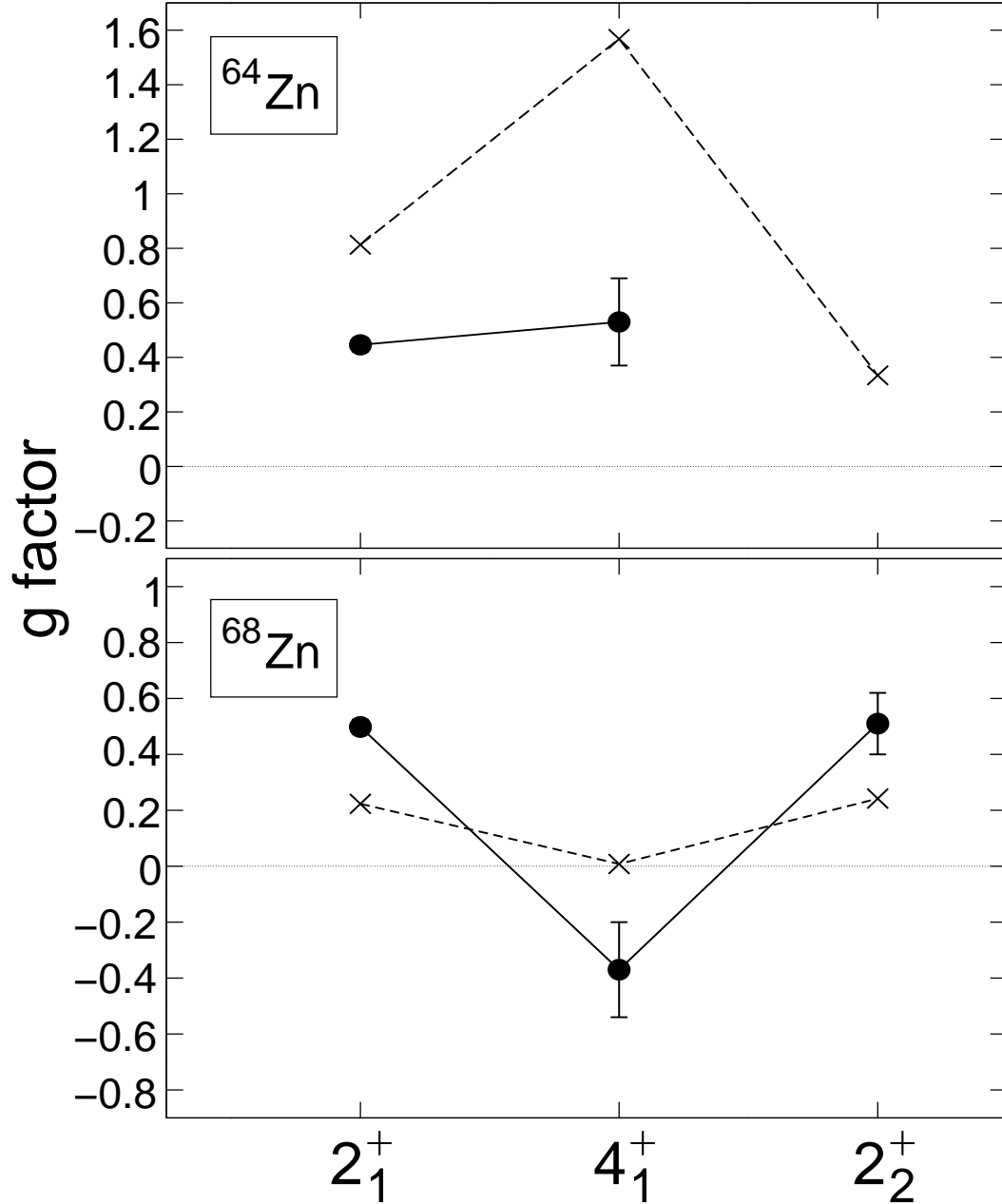


Fig. 3. Comparison of experimental g factors associated with the 2_1^+ , 4_1^+ and 2_2^+ states in ^{64}Zn and ^{68}Zn (closed circles) with results from large-scale shell model calculations (crosses, see text). Lines are drawn to guide the eye.

via many-body perturbation theory to third order, employing a renormalized nucleon-nucleon interaction defined for ^{56}Ni as closed shell core and including folded-diagrams to infinite order. For details, see for example Ref. [10]. A harmonic oscillator basis was used, with an oscillator energy determined via $\hbar\Omega = 45A^{-1/3} - 25A^{-2/3} = 10.1$ MeV, $A = 56$ being the mass number. For the single-particle energies we employ values adapted from Grawe in Ref. [12], resulting in the energy differences $\epsilon_{0g_{9/2}} - \epsilon_{1p_{3/2}} = 3.70$ MeV, $\epsilon_{0f_{5/2}} - \epsilon_{1p_{3/2}} =$

0.77 MeV, $\epsilon_{1p_{1/2}} - \epsilon_{1p_{3/2}} = 1.11$ MeV for neutrons and $\epsilon_{0g_{9/2}} - \epsilon_{1p_{3/2}} = 3.51$ MeV, $\epsilon_{0f_{5/2}} - \epsilon_{1p_{3/2}} = 1.03$ MeV, $\epsilon_{1p_{1/2}} - \epsilon_{1p_{3/2}} = 1.11$ MeV for protons. The effective interaction has not been corrected for any eventual monopole changes. This means that the only parameters which enter our calculations are those defining the nucleon-nucleon interaction fitted to reproduce the scattering data, the experimental single-particle energies and the oscillator basis. Furthermore, for the computation of the B(E2)'s and g factors, we have used unrenormalized magnetic moments and the canonical unrenormalized charges for protons and neutrons. The latter entails charges of $1.5e$ and $0.5e$ for protons and neutrons, respectively. The free-nucleon operator for the magnetic moment is defined as

$$\mu_{\text{free}} = g_l \mathbf{l} + g_s \mathbf{s}, \quad (4)$$

with $g_l(\text{proton}) = 1.0$, $g_l(\text{neutron}) = 0.0$, $g_s(\text{proton}) = 5.586$, $g_s(\text{neutron}) = -3.826$. Note, however, that the magnetic moment operator in finite nuclei is modified from the free-nucleon operator due to core-polarization and meson-exchange current (MEC) corrections [13,14]. The effective operator is defined as

$$\mu_{\text{eff}} = g_{l,\text{eff}} \mathbf{l} + g_{s,\text{eff}} \mathbf{s} + g_{p,\text{eff}} [Y_2, \mathbf{s}], \quad (5)$$

where $g_{x,\text{eff}} = g_x + \delta g_x$, $x = l, s$ or p , with g_x the free-nucleon, single-particle g factors ($g_p = 0$) and δg_x the calculated correction to it. Note the presence of a new term $[Y_2, \mathbf{s}]$, absent from the free-nucleon operator, which is a spherical harmonic of rank $\lambda' = 2$ coupled to a spin operator to form a spherical tensor of multipolarity $\lambda = 1$. In the calculations below we limit ourselves to a calculation with free operators only. An obvious modification of the latter is to use renormalized moments, as done in the recent work of Ref. [15] for nuclei in the ^{132}Sn mass region.

The results of the calculations for the energies of the low-lying excited states for both ^{64}Zn and ^{68}Zn in Table 2, while $B(E2; 2_1^+ \rightarrow 0_1^+)$, $B(E2; 2_2^+ \rightarrow 0_1^+)$ and $B(E2; 4_1^+ \rightarrow 2_1^+)$ and the g factors $g(2_1^+)$, $g(2_2^+)$ and $g(4_1^+)$ are presented and compared with the available data.

Two types of shell-model results are discussed and shown in this Table, SM-1 and SM-2. In SM-1 we limit the number of neutrons which can be excited to the $0g_{9/2}$ orbit to two, whereas SM-2 is the full shell-model calculation. The latter basis is, however, unnecessarily large since the results are converged with four neutrons at most in the $0g_{9/2}$ orbit. One sees clearly that with at most two neutrons in the $0g_{9/2}$ orbit the spectrum is rather poorly reproduced. However, even for the fully converged calculation the first excited 0_2^+ state at 1.655 MeV is badly reproduced ($E^{SM-2} = 2.406$ MeV), indicating most likely the need for particle-hole excitations, especially from the $0f_{7/2}$ orbit. The

typical occupation probabilities in the SM-2 calculation of the $0g_{9/2}$ neutron single-particle orbit span from 2.2 to 2.4. The $1p_{3/2}$ neutron orbit has an average occupancy of 3.5 particles whereas the low-lying $1f_{5/2}$ neutron orbit has occupancies around three. We note that for the 2_1^+ , 2_2^+ and the 4_1^+ states there is a satisfactory agreement with the data.

For ^{68}Zn the $B(E2;2_1^+ \rightarrow 0_1^+)$ exhibits a good agreement with data using unrenormalized effective charges while the $B(E2;4_1^+ \rightarrow 2_1^+)$ is overestimated. This could be ascribed to deficiencies in the two-body Hamiltonian and/or omitted degrees of freedom in the model space.

For ^{64}Zn we get $170.4 e^2\text{fm}^4$ for the $B(E2;2_1^+ \rightarrow 0_1^+)$, to be compared with the experimental value of $307 e^2\text{fm}^4$, hinting at the need of larger effective charges. This means in turn that particle-hole excitations involving the $0f_{7/2}$ orbit may be more important for ^{64}Zn than for ^{68}Zn , in good agreement with previous shell model calculations including this degree of freedom (see for example the discussions in Refs. [6,7]). This is also reflected in the g factors for ^{64}Zn , which tend to be larger than the experimental values. If we, however, introduce effective magnetic moments by assuming a renormalization factor of 0.7 – 0.8 for g_s of protons and neutrons, we obtain g factors closer to experiment. However, the $0f_{7/2}$ orbit, if coupled with the $1p_{3/2}$ orbit can yield a negative contribution to the g factors. The latter analysis is obviously performed at the level of a simple two-body configuration (see for example discussions in Refs. [16,17,18]), however, together with the $(0g_{9/2})^2$ configuration these are the only two-body configurations of interest here which can yield a negative g factor. For ^{64}Zn the occupancy of the $0g_{9/2}$ orbit is less than one, and plays therefore a negligible role in the calculation of g factors. Since excitations from the ^{56}Ni closed shell core are not included in the present model space, this reduction cannot be accounted for. Thus, the theoretical values should be larger than the experimental ones.

For ^{68}Zn and its g factors we note that for the 2^+ states there is a fair agreement with data, confirming the previous shell-model analysis presented in Refs. [6,7]. For $g(4_1^+)$ we see that there is again a change from the calculation with only two neutrons in the $0g_{9/2}$ orbit to the full calculation. This displays the role played by the $0g_{9/2}$ orbit, which for the 4_1^+ has an average occupation probability of 2.4 in the full SM-2 calculation, much larger than we have for ^{64}Zn . For SM-1 the corresponding occupation probability is 1.99 and this difference is clearly reflected in the change of $g(4_1^+)$ from 0.066 to 0.008 demonstrating thereby the dominating role played by the $(0g_{9/2})^2$ admixture in the wave function. However, for SM-2 the g factor although very small, is still positive. Introducing effective magnetic moments with a scaling factor of 0.7 reduces the theoretical SM-2 value to $g(4_1^+) = +0.003$. We speculate again whether particle-hole excitations involving the $0f_{7/2}$ orbit could yield further reductions and eventually a negative contribution. Furthermore, an-

other possibility is to include the effect of meson-exchange currents, as done in Ref. [15]. Meson-exchange current corrections arise because nucleons in nuclei are interacting through the exchange of mesons, which can be disturbed by the electromagnetic field. In terms of effective one-body operators this leads to a correction term $[Y_2, \mathbf{s}]$ in Eq. (5). In spite of these omitted degrees of freedom, we see that our model space displays the important role played by the $(0g_{9/2})^2$ neutron configuration when going from the SM-1 to the full SM-2 shell-model calculation, lending thereby support to the experimental analysis.

The role of the neutron $g_{9/2}$ orbit is also seen in the g factors of low-lying $9/2^+$ states in odd Zn isotopes with a large negative value, although smaller in absolute value than the corresponding Schmidt value (see Ref. [19]).

4 Summary and conclusions

We have remeasured the g factor of the 4_1^+ state in ^{68}Zn , with an improved energy resolution of the detectors used. The experimental value is $g(4_1^+) = -0.37(17)$ consistent with our previous measurements. In addition, the accuracy of the g factors of the 2_1^+ , 2_2^+ and 3_1^- states has been improved and their lifetimes were well reproduced. The experimental results for ^{64}Zn and ^{68}Zn have been compared with large-scale shell model calculations using ^{56}Ni as a closed shell core and a model space consisting of protons and neutrons occupying the $0f_{5/2}1pg_{9/2}$ single-particle orbits. The agreement between theory and experiment is rather good and the calculations reproduce well the experimental trends for the g factors from ^{64}Zn to ^{68}Zn , although our theoretical approach is not capable of reproducing the negative sign of the $g(4_1^+)$ value in ^{68}Zn . This deficiency may be ascribed to particle-hole excitations, with the $0f_{7/2}$ orbit playing a major role. The effect of meson-exchange currents may also play a role and will be investigated in future works, together with the inclusion of the $0f_{7/2}$ orbit. In view of the present results similar measurements for the Ge isotones ^{66}Ge and ^{70}Ge are highly desirable to search for corresponding effects in the nuclear wave functions.

Acknowledgements

The authors are thankful to the operating staff of the Munich tandem accelerator. Support by the BMBF and the Deutsche Forschungsgemeinschaft is acknowledged. The work of TE and MHJ has been supported by the Research Council of Norway (Program for Supercomputing) through a grant of computing time. Discussions with Alex Brown (MSU) and Georgi Georgiev (CERN) are gratefully acknowledged.

References

- [1] R. V. F. Janssens and T. L. Khoo, *Ann. Rev. Nucl. Part. Sci.* **41** (1999) 321
- [2] T. Sakuda and S. Ohkubo, *Nucl. Phys. A* **744** (2004) 77
- [3] E. Ideguchi *et al.*, *Phys. Rev. Lett.* **87** (2001) 222501
- [4] C. E. Svensson *et al.*, *Phys. Rev. Lett.* **82** (1999) 3400
- [5] C. E. Svensson *et al.*, *Phys. Rev. Lett.* **79** (1997) 1233
- [6] O. Kenn *et al.*, *Phys. Rev. C* **65** (2002) 034308
- [7] J. Leske, K.-H. Speidel, S. Schielke, O. Kenn, D. Hohn, J. Gerber, and P. Maier-Komor, *Phys. Rev. C* **71** (2005) 034303
- [8] Huo Junde and B. Singh, *Nucl. Data Sheets* **91** (2000) 395
- [9] J. C. Wells and N. R. Johnson, program LINESHAPE, 1994, Oak Ridge National Laboratory, (unpublished)
- [10] M. Hjorth-Jensen, T. T. S. Kuo, and E. Osnes, *Phys. Rep.* **261** (1995) 125
- [11] R. Machleidt, *Phys. Rev. C* **63** (2001) 024001
- [12] H. Grawe, M. Gorska, M. Rejmund, M. Pfützner, M. Lipoglavsek, C. Fahlander, M. Hellström, D. Kast, A. Jungclaus, K. P. Lieb, R. Grzywacz, K. Rykaczewski, B. A. Brown, M. Hjorth-Jensen, and K. H. Maier, in *Highlights of Modern Nuclear Structure*, Ed. A. Covello, (World Scientific, Singapore, 1999), p. 137.
- [13] I.S. Towner, *Phys. Rep.* **185** (1987) 263
- [14] B. Castel and I. S. Towner, *Modern Theories of Nuclear Moments*, (Clarendon, Oxford, 1990).
- [15] B. A. Brown, N. J. Stone, J. R. Stone, I. S. Towner, and M. Hjorth-Jensen, *Phys. Rev. C* **71** (2005) 044317
- [16] R. D. Lawson, *Theory of the Nuclear Shell Model*, (Clarendon Press, Oxford, 1980), pp. 295-316.
- [17] A. Arima and H. Horie, *Prog. Theor. Phys.* **11** (1954) 509
- [18] G. Georgiev, PhD thesis, University of Leuven, Belgium, unpublished (2001)
- [19] P. Herzog *et al.*, *Z. Phys. A* **332** (1989) 247